Intercalation of Aminophenyl- and Pyridinium-Substituted Porphyrins into Zirconium Hydrogen Phosphate: Evidence for Substituent-Derived Orientational Selectivity

Ronald M. Kim, John E. Pillion, David A. Burwell, John T. Groves,* and Mark E. Thompson*

Department of Chemistry, Princeton University, Princeton, New Jersey 08544

*Received June 15, 1993**

Aminophenyl- and pyridinium-substituted porphyrins were intercalated into the α phase of zirconium hydrogen phosphate (α-ZrP) by exchanging the porphyrins into the *p*-methoxyaniline (PMA) preintercalated compound $Zr(O_3POH)_2 \cdot 2PMA$ (α-ZrP·2PMA). Porphyrin exchange reactions with α-ZrP and its ethanol intercalate were unsuccessful. Powder X-ray diffraction patterns of *p*-H_2TAPP- and H_2TMPyP-exchanged α-ZrP·2PMA revealed complete conversion of the starting material to phases with interlayer spacings near 17 Å, corresponding to a guest layer thickness of ca. 11 Å. The *p*-H_2TAPP derivative was found to partially convert over several weeks to α-ZrP and a 24-Å phase material. The large interlayer spacing cannot be accounted for by a porphyrin monolayer and is tentatively assigned to a porphyrin bilayer in which the heme planes are tilted relative to the host lamellae. Conversely, intercalation of α-ZrP·2PMA with the $\alpha,\alpha,\alpha,\alpha$, $\alpha,\alpha,\alpha,\beta$, and $\alpha,\beta,\alpha,\beta$ atropisomers of *o*-H_2TAPP afforded multiphasic products with interlayer spacings of 13, 17, 19–20, and 25 Å. The relative intensities of the phases were highly dependent on the atropisomer, with the $\alpha,\alpha,\alpha,\alpha$ isomer forming mainly a 19-Å phase and *o*-$\alpha,\beta,\alpha,\beta$-$H_2$TAPP forming predominantly a 17-Å phase. In order to determine the orientations of porphyrins comprising the 17- and 19–20-Å phases relative to the host lamellae, *p*-CuTAPP and *o*-$\alpha,\alpha,\alpha,\alpha$-CuTAPP intercalation complexes were prepared, and anisotropic EPR spectra of uniaxially ordered thin films oriented at 0 and 90° relative to the applied magnetic field were recorded. The EPR spectra of the *p*-CuTAPP-exchanged host displayed little orientational dependence, consistent with tilting of the heme macrocycles near 45° relative to the host lamellae. Conversely, the EPR spectra of uniaxially ordered films of the *o*-$\alpha,\alpha,\alpha,\alpha$-CuTAPP-exchanged host exhibited a strong orientation dependence, with the perpendicular component of the Cu(II) signal dominating the spectrum in samples oriented at 90° relative to B_0 and the parallel component predominating in films oriented at 0° relative to B_0, indicating that the porphyrins were highly oriented parallel to the host layers. Together, the XRD and EPR data suggest that the guest morphology of the *p*-TAPP derivatives consisted of a monomolecular porphyrin layer in which the heme planes were tilted nearly 45° relative to the host lamellae, whereas *o*-$\alpha,\alpha,\alpha,\alpha$-TAPP derivatives predominantly assembled into a porphyrin bilayer in which the heme macrocycles lay parallel with the host sheets. The preferred porphyrin orientations are discussed in terms of maximization of electrostatic and hydrogen-bonding interactions between the host and guest.

Introduction

Layered inorganic materials such as clays, dichalcogenides, and metal phosphates have been extensively studied due to their catalytic activity, ion-exchange capacity, and stability.[1] The ability of these materials to incorporate guest molecules has led to growing interest in their use as frameworks for the formation of highly ordered assemblies whose structures may be tailored at the molecular level through the design of the host or the guest. Incorporation of guest molecules into layered hosts has been utilized in the design of such diverse materials as catalysts,[2] conducting polymers,[3] energy storage devices,[4] and receptors.[5] The insertion of porphyrins and metalloporphyrins into ordered matrices are of interest due to their oxygen-binding and catalytic activity, as well as their photoactive and conductive properties. We recently reported the synthesis of a membrane-spanning porphyrin which inserts into phospholipid bilayers with the heme macrocycle poised at the membrane core and oriented perpendicular to the bilayer normal, anchored by four steroid appendages.[6] The highly ordered porphyrin microenvironment was shown to direct highly regioselective oxidation of steroid and unsaturated fatty acid substrates.

The intercalation of layered host structures with porphyrins has previously been accomplished in aluminosilicates. Cady and Pinnavaia have reported the intercalation of tetraphenylporphyrin (H_2TPP) in montmorillonite.[7] Kameyama and co-workers inserted CoTMPyP into montmorillonite.[8] Carrado and Winans ion-exchanged tetrakis(*N*-methylpyridinium-4-yl)porphyrin (H_2-TMPyP) and tetrakis(4-(trimethylamino)phenyl)porphyrin (H_2-TMAPP), and the corresponding Fe and Co metalloporphyrins, into montmorillonite and low-charge fluorohectorite.[9] Giannelis reported intercalation of CuTMPyP in hectorite and high-charge fluorohectorite.[10] Recently, Mansuy and co-workers synthesized supported catalysts composed of MnTMPyP-intercalated mont-

* Abstract published in *Advance ACS Abstracts,* September 15, 1993.

(1) (a) *Intercalation Chemistry*; Whittingham, M. S., Jacobson, A. J., Eds.; Academic Press: New York, 1982. (b) Clearfield, A. *Chem. Rev.* **1988**, *88*, 125. (c) Alberti, G.; Costantino, U. In *Inorganic and Physical Aspects of Inclusion*; Atwood, J. L., Davies, J. E. D., MacNicol, D. D., Eds.; Inclusion Compounds, Vol. 5; Oxford University Press: New York; 1991.

(2) (a) Pinnavaia, T. J.; Welty, P. K. *J. Am. Chem. Soc.* **1975**, *97*, 3819. (b) Iwamoto, M.; Nomura, Y.; Kagawa, S. *J. Catal.* **1981**, *69*, 234. (c) Clearfield, A.; Thakur, D. S.; Cheung, H. *J. Phys. Chem.* **1982**, *86*, 500. (d) Pinnavaia, T. J.; Tzou, M. S.; Landau, S. D. *J. Am. Chem. Soc.* **1985**, *107*, 4783.

(3) (a) Kanatzidiz, G.; Marcy, H.; McCarthy, W. J.; Kannewurf, C. R.; Marks, T. J. *Solid State Ionics* **1989**, *32/33*, 594. (b) Mehotra, V.; Giannelis, E. P. *Solid State Commun.* **1991**,*77*, 155.

(4) (a) Vermeulen, L. A.; Thompson, M. E. *Nature,* **1992**, *358*, 656. (b) Rouxel, J.; Brec, R. *Annu. Rev. Mater. Sci.* **1986**, *16*, 137. (c) Pasquariello, D. M.; Abraham, K. M. *Mater. Res. Bull.* **1987**, *22*, 37.

(5) (a) Johnson, J. W.; Jacobson, A. J.; Butler, W. M.; Rosenthal, S. E.; Brody, J. F.; Lewandowski, J. T. *J. Am. Chem. Soc.* **1989**, *111*, 381. (b) Cao, G.; Mallouk, T. E. *Inorg. Chem.* **1991**, *30*, 1434.

(6) (a) Groves, J. T.; Neumann, R. *J. Am. Chem. Soc.* **1987**, *109*, 5045. (b) Groves, J. T.; Neumann, R. *J. Org. Chem.* **1988**, *53*, 3891. (c) Groves, J. T.; Neumann, R. *J. Am. Chem. Soc.* **1989**, *111*, 2900.

(7) Cady, S. S.; Pinnavaia, T. J. *Inorg. Chem.* **1978**, *17*, 1501.

(8) Kameyama, H.; Suzuki, H.; Amano, A. *Chem. Lett.* **1988**, 1117.

(9) Carrado, K. A.; Winans, R. E. *Chem. Mater.* **1990**, *2*, 328.

(10) Giannelis, E. P. *Chem. Mater.* **1990**, *2*, 627.

(11) Barloy, L.; Lallier, J. P.; Battioni, P.; Mansuy, D.; Piffard, Y.; Tournoux, M.; Valim, J. B.; Jones, W. *New J. Chem.* **1992**, *16*, 71.

0020-1669/93/1332-4509$04.00/0

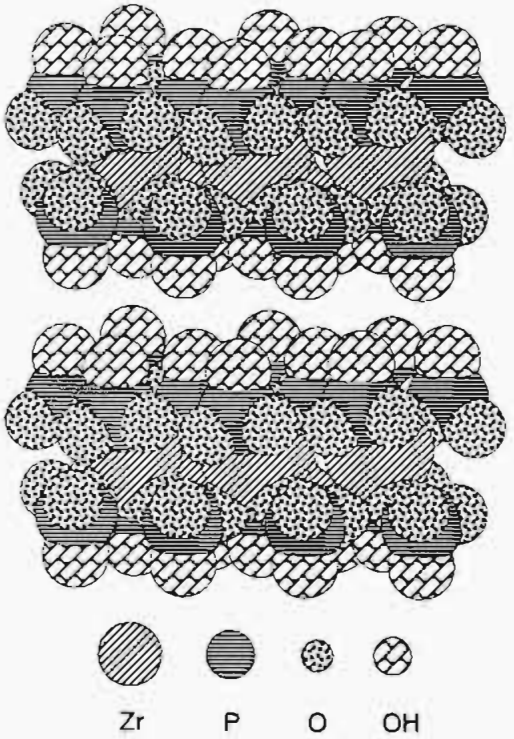

Figure 1. Structure of α-ZrP.

morillonite.[11] In the forementioned assemblies, the porphyrin orientations were dictated by the density of charged groups in the host. Due to the relatively low silicate density of montmorillonite and hectorite, intercalated porphyrins adopted orientations parallel to the host layers. Conversely, CuTMPyP in fluorohectorite was canted relative to the silicate layers.[9] The canted orientation was ascribed to the higher density of the silicate anions in fluorohectorite, and the compensatory tilting of the intercalated porphyrins in order to increase the packing of cationic pyridinium groups, thereby balancing the host charges.

During the time of our investigation, Katz, Ungashe, and coworkers reported the assembly of thin films composed of alternating porphyrin and viologen zirconium phosphonate layers.[12] Interestingly, photoinduced electron transfer from the porphyrin to the viologen layer was found to take place through the intervening zirconium atoms. To date, however, intercalation of porphyrins into bulk α-zirconium hydrogen phosphate has not been reported.

The α phase of zirconium hydrogen phosphate, $Zr(O_3POH)_2{\cdot}H_2O$ (α-ZrP), has received much attention as a layered inorganic host.[13] As depicted in Figure 1, the solid consists of stacked sheets of zirconium atoms bridged by phosphate groups, which are held together by van der Waals interactions. As a result of the weak interlayer interactions, guest molecules can insert between the layers, causing the sheets to separate, affording an intercalated complex consisting of alternating host and guest layers. A number of organic, inorganic, and organometallic guest molecules have been intercalated into α-ZrP, most commonly via ion exchange or acid–base reactions with the acidic phosphates. Due to their high basicity, amines are especially effective guests.[14] Recently, oxidation–reduction[15] as well as esterification and

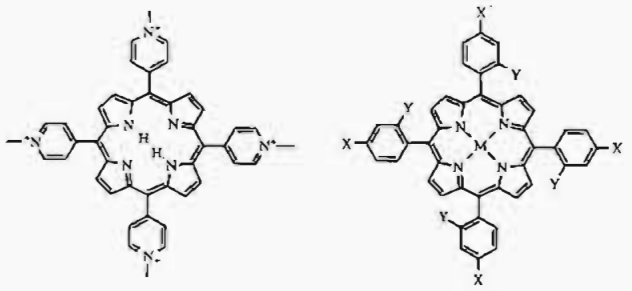

H_2TMPyP

X=NH_2, Y=H, M=H_2: *p*-H_2TAPP
X=NH_2, Y=H, M=Cu: *p*-CuTAPP

X=H, Y=NH_2, M=H_2: *o*-H_2TAPP

Figure 2. Structures of porphyrins used in this study.

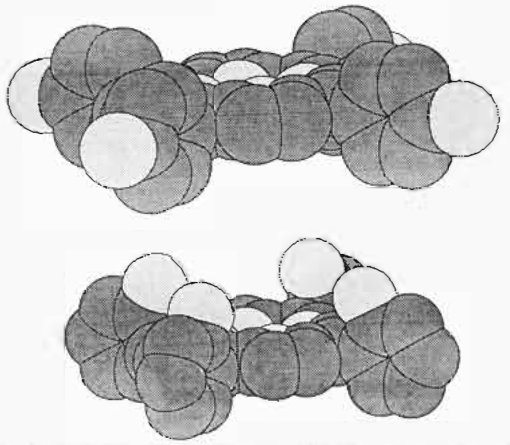

Figure 3. Space-filling representations (hydrogens omitted) of *p*-H_2TAPP (top) and *o*-$\alpha,\alpha,\alpha,\alpha$-$H_2$TAPP (bottom).

amidation reactions[16] have also been used to drive intercalation of guest molecules into α-ZrP and related layered hosts.

Our efforts have centered on intercalating *N*-methylpyridinium and various aminophenyl-substituted porphyrins into bulk α-ZrP. The porphyrins used in this study are depicted in Figure 2. In contrast to the previously mentioned studies of porphyrin-intercalated aluminosilicates, in which the orientation of the porphyrins was dictated by the charge density of the hosts, a primary goal of our investigation was to predictably control the morphologies of porphyrin assemblies in α-ZrP via design of simple porphyrin guests. We postulated that amino and pyridinium substituents residing on the meso phenyl groups of TPP-type porphyrins would direct the orientation of the porphyrins in α-ZrP by maximizing electrostatic and hydrogen-bonding interactions with the host phosphates, and possibly allow for porphyrin π-stacking interactions. As can be seen from the space-filling representations of *p*-H_2TAPP and *o*-$\alpha,\alpha,\alpha,\alpha$-$H_2$TAPP presented in Figure 3, the directionality of substituents situated at the ortho and para phenyl positions differ greatly relative to the heme macrocycle. Thus, we anticipated that amino and pyridinium substituents could be utilized to direct the formation of intercalation complexes in which the orientations of the porphyrin macrocycles differed relative to the ZrP layers. In addition to differences in the directionality of *ortho* and *para* substituents relative to the heme plane, the different distribution of amines per porphyrin face of different *o*-H_2TAPP atropisomers could also lead to the assembly of different porphyrin structures. Powder X-ray and EPR spectra of the porphyrin intercalation complexes indeed indicate that the positions of substituents on the *meso*

(12) Ungashe, S. B.; Wilson, W. L.; Katz, H. E.; Scheller, G. R.; Putvinski, T. M. *J. Am. Chem. Soc.* **1992**, *114*, 8717.
(13) (a) Clearfield, A.; Stynes, J. A. *J. Inorg. Nucl. Chem.* **1964**, *26*, 117. (b) Clearfield, A. *Chem. Rev.* **1988**, *88*, 125. (c) Alberti, G.; Costantino, U., In *Inorganic and Physical Aspects of Inclusion*; Atwood, J. L., Davies, J. E. D., MacNicol, D. D., Eds.; Inclusion Compounds, Vol. 5; Oxford University Press: New York, 1991.
(14) (a) Michel, E.; Weiss, A. *Z. Naturforsch., B* **1965**, *20*, 1307. (b) Costantino, U. *J. Chem. Soc., Dalton Trans.* **1979**, 402. (c) Clearfield, A.; Twinda, R. M. *J. Inorg. Nucl. Chem.* **1979**, *41*, 871.
(15) Johnson, J. W. *J. Chem. Soc., Chem. Commun.* **1980**, 263.
(16) (a) Ortiz-Avila, C. Y.; Clearfield, A. *Inorg. Chem.* **1985**, *24*, 1773. (b) Burwell, D. A.; Thompson, M. E. *Chem. Mater.* **1991**, *3*, 730.

phenyl groups, as well as the distribution of ortho amino groups on each porphyrin face, direct the assembly of different guest structures.

Results

Intercalation of *p*-H_2TAPP and H_2TMPyP into α-ZrP. α-$Zr(O_3POH)_2 \cdot H_2O$ is an ideal host for the intercalation of organic amines. Alkylamines react with α-ZrP *via* Brønsted acid–base reactions to give an intercalation compound $[Zr(O_3PO^-)_2(RNH_3^+)_2]$, which is composed of alternating layers of $Zr(O_3PO^-)_2$ and bilayers of RNH_3^+. Weakly basic or sterically hindered amines do not react directly with α-ZrP to give fully intercalated materials; however, formation of a metastable ethanol intercalate, $Zr(O_3POH)_2(EtOH)_n$,[17] prior to treatment with the weakly basic amine can lead to fully intercalated materials.[18] While the ethanol intercalation compound seems ideal for the preparation intercalation compounds with *p*-H_2TAPP and *o*-H_2TAPP guests, there are difficulties associated with this approach. The ethanol intercalation compound readily loses ethanol and must be prepared freshly each time it is used. In addition, the ethanol intercalation compound will not engage in ion-exchange reactions, precluding its use for H_2TMPyP guests. Both α-ZrP and its ethanol intercalate failed to intercalate *p*-H_2TAPP and H_2TMPyP from a variety of solvents. The disodium salt $Zr(O_3PONa)_2 \cdot 3H_2O$ (α-ZrP·2Na) appeared to incorporate both *p*-H_2TAPP and H_2TMPyP to a very small extent, as indicated by weak, broad reflections in the powder X-ray diffraction (XRD) patterns near 18, 12, and 11 Å.[19] The inability of α-ZrP to accommodate the porphyrins to a high degree was presumably a consequence of the large surface area of the porphyrin per exchangeable group (i.e. amino and pyridinium moieties) and the weak basicity of the anilino nitrogens of *p*-H_2TAPP.

In order to overcome the energetic barrier required to separate the zirconium layers upon porphyrin intercalation, porphyrin-exchange reactions with the *p*-methoxyaniline-preintercalated complex $Zr(O_3POH)_2 \cdot 2CH_3OC_6H_4NH_2$ (α-ZrP·2PMA) were investigated. We anticipated that α-ZrP·2PMA would be an excellent starting material for intercalation of bulky and/or weakly basic guests, in that it combines a large interlayer spacing (ca. 22 Å) with readily exchangeable aniline guests. Furthermore, unlike alcohol-preintercalated complexes, α-ZrP·2PMA is quite stable; the solid used in this study had been prepared 2 years prior and stored under ambient conditions. XRD revealed only slight decomposition of the solid in this time, with minor impurity phases at 20.0, 16.9, and 14.9 Å, in addition to the predominant phase at 21.7 Å (Figure 4a). The 21.7-Å interlayer spacing of α-ZrP·2PMA corresponds to a gallery height of 15.4 Å (the thickness of an α-ZrP layer is 6.3 Å), which is consistent with a bilayer assembly in which the long PMA axis lies roughly 60° to the host layers. Elemental and thermogravimetric analyses also support a bilayer assembly.

Addition of α-ZrP·2PMA to a solution of *p*-H_2TAPP dissolved in ethanol resulted in decolorization of the solvent and darkening of the solid, indicating uptake of the porphyrin chromophore from solution by the host. Intercalation of ca. 300 μmol of porphyrin/g of α-ZrP·2PMA, or one porphyrin per six zirconium atoms, was determined by monitoring the decrease in the visible absorbance of the porphyrin in solution. The stoichiometry of the reaction clearly cannot be accounted for by surface adsorption and must therefore involve incorporation of porphyrin into the host matrix (i.e. intercalation). Uptake of porphyrin from solution was initially quite rapid, reaching equilibrium in a matter of minutes. GC analysis of the solution indicated the release of 3.1

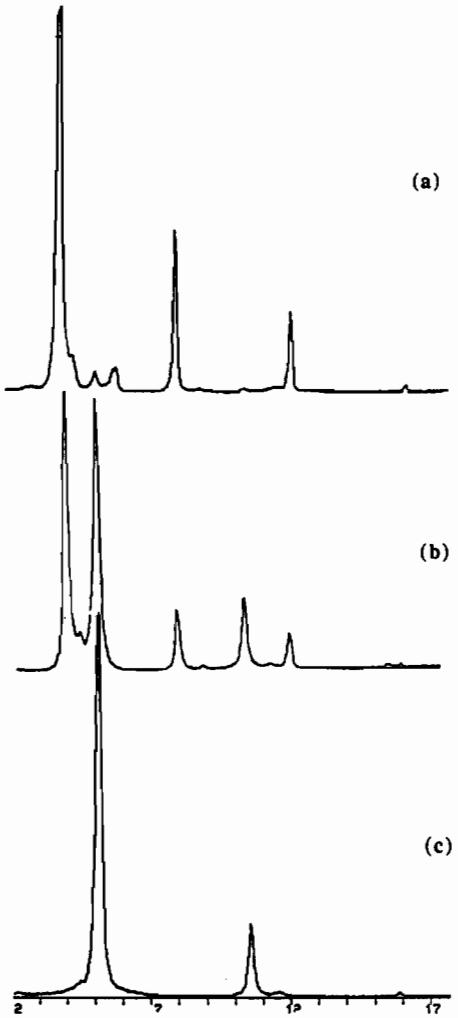

Figure 4. XRD patterns of (a) α-ZrP·2PMA, (b) partially *p*-H_2TAPP-exchanged α-Zr·2PMA, and (c) "fully" *p*-H_2TAPP-exchanged α-Zr·2PMA. Horizontal axis is in degrees 2θ.

PMA molecules from the host per intercalated porphyrin, which correlates well with the presence of four amino groups per porphyrin. This value represents a lower limit, since PMA was later found to degrade in solution in the presence of porphyrin. The porphyrin-exchanged solid was found to partially deintercalate in chloroform.

XRD patterns of the starting material and of partially and "fully" porphyrin-exchanged α-ZrP·2PMA are displayed in Figures 4b,c. The formation of a new phase with an interlayer spacing of 17.0 Å, and the concomitant disappearance of the starting material at 21.7 Å, are evident. The spectrum of the "fully" intercalated host illustrates the complete conversion of starting material to the porphyrin-intercalated phase, as well as high crystallinity of the heme derivative. The 17.0-Å interlayer spacing corresponds to a guest occupation of 10.7 Å, which is consistent either with a monomolecular porphyrin layer in which the heme planes are canted relative to the host lamellae (Figure 5a) or with a porphyrin bilayer in which the hemes lie roughly parallel with the host sheets (Figure 5b). Assuming a porphyrin edge distance (the distance between amines on adjacent phenyl groups) of 15 Å, a monolayer assembly corresponds to a tilt angle of approximately 45° relative to the host sheets. The gallery height is very close to that reported for CuTMPyP-intercalated fluorohectorite.[10] Noteworthy are the similar charge densities of the fluorohectorite[10] and α-ZrP, of 27 and 24 Å^2 per OH site, respectively.

XRD patterns of the fully *p*-H_2TAPP-intercalated complex stored over several weeks revealed partial conversion of the 17-Å phase to a 24-Å phase and to deintercalated α-ZrP. The 24-Å

(17) Costantino, U. *J. Chem. Soc., Dalton Trans.* **1979**, 402.
(18) (a) Chatakondu, K.; Formstone, C.; Green, M. L. H; O'Hare, D.; Twyman, J. M.; Wiseman, P. J. *J. Mater. Chem.* **1991**, *1*, 205. (b) Szirtes, L.; Kőrnyei, J.; Pokó, Z. *React Polym.* **1988**, *7*, 185.
(19) Burwell, D. A. Ph.D. Thesis, Princetion University, Jan 1992.

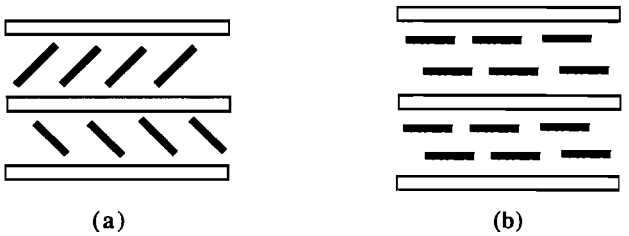

Figure 5. Stylized depictions of (a) a canted porphyrin monolayer and (b) a planar porphyrin bilayer.

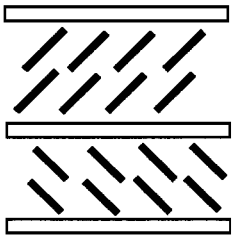

Figure 6. Stylized representation of a canted porphyrin bilayer.

interlayer spacing corresponds to a gallery height of 18 Å, which is too large to be accounted for by a heme monolayer and is tentatively ascribed to a porphyrin bilayer in which the hemes are canted relative to the host layers, as depicted in Figure 6. Attempts to form the 24-Å phase directly by performing intercalation reactions with a large excess of *p*-H_2TAPP and longer reaction times were unsuccessful, affording only the 17-Å phase. Reorganization over time to the 24-Å phase suggests that the canted monolayer may be a kinetically favored structure, which gradually converts to the thermodynamically favored canted bilayer.

Intercalation reactions between α-ZrP·2PMA and the chloride and tosylate salts of H_2TMPyP were performed in EtOH/H_2O. UV spectroscopy revealed that intercalation of H_2TMPyP was not as rapid as uptake of *p*-H_2TAPP, with the tosylate salt reaching equilibrium in approximately 3 h and the chloride derivative taking somewhat longer. The slower exchange rates may reflect a weaker driving force for intercalation due to the absence of hydrogen bonding between the host and the pyridinium guests. The stoichiometries of the reactions were similar to that observed upon intercalation of *p*-H_2TAPP. XRD patterns of the chloride and tosylate salts showed clean conversion to a porphyrin-intercalated phase at 16.9 Å. The similarity in layer spacings of the H_2TMPyP-intercalated complex and of *p*-H_2TAPP-exchanged α-ZrP·2PMA is suggestive of similar orientations adopted by the porphyrin guests, which are consistent with either a canted monolayer or planar bilayer assembly (Figure 5).

Intercalation of α-ZrP·2PMA with *o*-H_2TAPP Atropisomers. *o*-H_2TAPP consists of a statistical mixture of four rotational isomers: α,α,α,α, α,α,α,β, α,β,α,β, and α,α,β,β (α and β denote the respective porphyrin faces toward which the amino functionalities reside). The atropisomers are interconvertible via rotation of the *meso* phenyl groups. This rotation is sterically hindered by the ortho amino substituents, and the atropisomers are therefore readily isolable, reisomerizing in the time scale of days in solution at room temperature. The isomers are more stable in the solid phase.

Reactions between α-ZrP·2PMA and the α,β,α,β, α,α,α,β, and α,α,α,α rotamers of *o*-H_2TAPP were carried out in acetone for 2–3 days. TLC of the reaction solutions indicated that little interconversion of the atropisomers had occurred in this time. In contrast to the single-phased intercalation complexes initially obtained using the para-substituted porphyrins, the *o*-H_2TAPP intercalation compounds were composed of multiple phases, as revealed by XRD (Figure 7). Interlayer spacings of 17 and 25 Å were present for all three atropisomers, similar to those observed for *p*-TAPP-exchanged α-Zr·2PMA, and may reflect the assembly

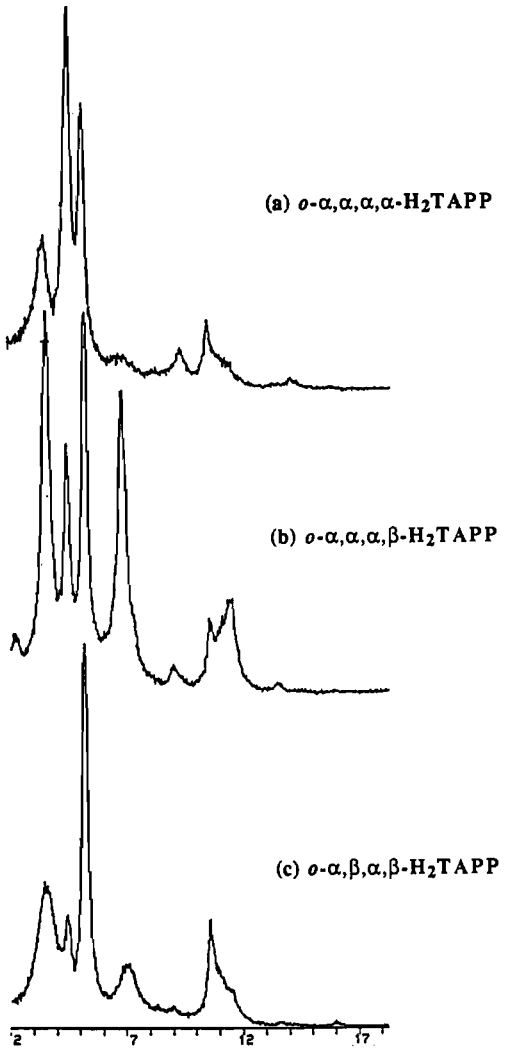

Figure 7. XRD patterns of α-ZrP·2PMA intercalated with (a) *o*-α,α,α,α-H_2TAPP, (b) *o*-α,α,α,β-H_2TAPP, and (c) *o*-α,β,α,β-H_2TAPP. Horizontal axis is in degrees 2θ.

of analogous guest structures. Additional phases were also present at 13 and 19–20 Å, in addition to reflections corresponding to fully deintercalated α-ZrP at 7.6 Å. No reflections corresponding to the PMA-intercalated starting material were observed. The 19–20-Å interlayer spacing corresponds to a gallery height of approximately 13 Å, which is suggestive of either a canted porphyrin monolayer or a planar bilayer assembly (Figure 5). The 12.5- and 12.8-Å phases observed in the α,α,α,β and α,β,α,β intercalation compounds correspond to gallery heights of 6.2 and 6.5 Å, respectively, and could arise from a monomolecular guest layer in which the heme planes lie roughly parallel with the host lamellae. The spacings are larger than those determined for planar porphyrin monolayers in montmorillonite and hectorite, as well as *p*-H_2TAPP-intercalated α-ZrP·2Na, but may be accounted for by the presence of amino substituents at the ortho positions of the meso phenyl groups, which lie roughly perpendicular to the porphyrin plane and therefore dictate the gallery height for porphyrins oriented parallel to the phosphate layers. The possibility that the 13-Å phase is actually a *d*(002) reflection corresponding to the *d*(001) reflection at 25 Å, however, cannot be ruled out on the basis of the X-ray data. The relative intensities of the various phases varied greatly depending on the atropisomer; a 19-Å phase predominated in the α,α,α,α-H_2TAPP derivative, whereas the α,β,α,β atropisomer displayed mainly a 17-Å phase. The interlayer spacings of the various porphyrin intercalates are listed in the Table I, with the predominant phase(s) shown in boldface.

Table I. Interlayer Spacings and Structure Assignments Determined from *d*(001) XRD Reflections of Porphyrin-Intercalated α-ZrP·2PMA (Predominant Phases Boldfaced)[a-g]

p-H_2TAPP[f]	*p*-H_2TAPP[g]	*o*-α,α,α,α-H_2TAPP	*o*-α,α,α,β-H_2TAPP	*o*-α,β,α,β-H_2TAPP	H_2TMPyP
	24.2[a]	24.7[a]	**24.5**[a]	24.7[a]	
		18.9[b]	19.7[b]	19.7[b]	
16.8[c]	**16.1**[c]	16.7[c]	**16.7**[c]	**16.7**[c]	**16.9**[c]
			12.8[d]	12.5[d]	
	7.7[e]		7.7[e]	7.6[e]	

[a-g] Structure assignments: (*a*) canted bilayer; (*b*) planar bilayer; (*c*) canted monolayer; (*d*) planar monolayer; (*e*) α-ZrP. [f] XRD recorded within 48 h of intercalation reaction. [g] XRD recorded after storage of intercalated solid for several weeks.

Several factors suggest that the 19–20-Å phase arises from a *planar porphyrin bilayer assembly*. The corresponding gallery height of ca. 13 Å is twice the 6.5-Å gallery height of the *o*-α,α,α,β-H_2TAPP intercalate, which we tentatively attribute to a planar porphyrin monolayer. The interlayer spacing of 18.9 Å observed for the α,α,α,α isomer is also somewhat smaller than the corresponding 19.7-Å separation measured for the α,α,α,β and α,β,α,β intercalation complexes, consistent with the presence of amino groups on only one face of the α,α,α,α rotamer, which would allow for tighter packing of the porphyrins, and thus a smaller gallery height. In addition, only the α,α,α,α intercalate afforded predominantly the 19-Å phase, which is reasonable considering that a planar bilayer assembly of the α,α,α,α atropisomer could produce twice as many as eight amine–phosphate interactions per porphyrin pair, compared with a maximum of six and four interactions per pair of the α,α,α,β and α,β,α,β atropisomers, respectively.

Intercalation of α-ZrP·2PMA with *p*-CuTAPP and *o*-α,α,α,α-CuTAPP. In order to distinguish between possible orientations of porphyrins comprising the 17- and 19-Å phases relative to the host lamellae of α-ZrP, *p*-CuTAPP and *o*-α,α,α,α-CuTAPP intercalation complexes of α-ZrP·2PMA were prepared. The anisotropic EPR signal of Cu(II) porphyrins has been utilized to determine their orientations in ordered matrices such as lipid multilayers,[6c,20] liquid crystals,[21] clays,[10] single crystals,[22] and Langmuir–Blodgett films.[23] Cu(II) porphyrins display an axially symmetric EPR signal, with a perpendicular component ($g_\perp$) lying in the porphyrin (xy) plane, and a parallel component ($g_\parallel$) along the *z* axis. As a result, the EPR spectra of copper porphyrins are dependent on the orientation of the heme relative to the applied magnetic field, B_0. EPR spectra of randomly ordered samples, or samples oriented such that B_0 is not parallel or perpendicular to the porphyrin plane, display both $g_\perp$ and $g_\parallel$ components. However, only $g_\parallel$ is observed for samples in which the Cu porphyrins are aligned perpendicular to B_0, due to quantization of the electron spin along the *z* axis, whereas $g_\perp$ is observed in samples oriented with the porphyrin planes parallel to B_0.

Intercalations of the Cu porphyrins were performed in acetone. As with the *p*-H_2TAPP derivative, the XRD pattern of the *p*-CuTAPP intercalate displayed predominantly a 17-Å interlayer spacing, presumably corresponding to an analogous porphyrin orientation. Uniaxially ordered samples were prepared by casting a slurry of Cu porphyrin-intercalated α-ZrP·2PMA onto glass cover slips and drying the samples in air to form thin films. Oriented thin films of α-ZrP complexes, as well as other layered inorganic solids, are readily formed due to the platelike morphology of the crystallites.[24] Thin films of α-ZrP orient such that the crystallites (and the host lamellae) lie parallel to the glass surface, (as depicted in Figure 8).

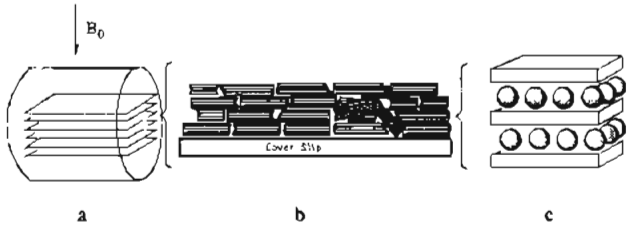

Figure 8. Schematic depiction of (a) oriented glass slides in an EPR tube, (b) side view of ZrP crystallites on a glass slide, and (c) layered lattice structure within a single crystallite.

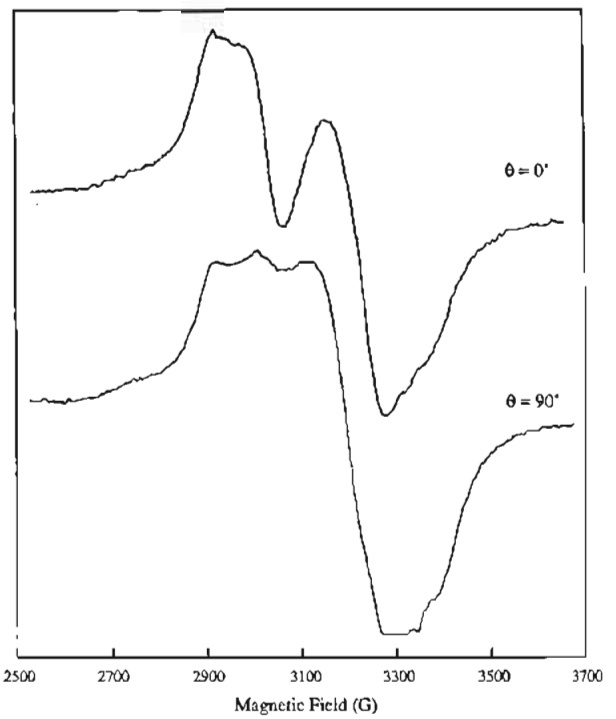

Figure 9. EPR spectra of uniaxially oriented films of *p*-CuTAPP-intercalated α-ZrP·2PMA oriented parallel (top) and perpendicular (bottom) to the magnetic field.

An assembly in which the Cu porphyrins lie parallel to the phosphate layers (e.g. a planar bilayer, Figure 5b), would show a strong orientational dependence in the EPR spectra, with samples oriented perpendicular to the applied magnetic field ($\theta = 90°$) displaying the perpendicular component and films oriented parallel to B_0 ($\theta = 0°$) displaying $g_\perp$. Conversely, for an assembly in which the Cu porphyrins are tilted nearly 45° relative to the host layers (e.g. a canted bilayer, Figure 5a), the EPR spectra of uniaxially ordered samples would be orientation independent, since the molecular environments experienced by the magnetic field would be similar regardless of the orientation of the film.[9,25] Similar spectra would therefore be obtained at $\theta = 0$ and 90°, with both perpendicular and parallel components appearing at the two orientations.

EPR spectra of uniaxially oriented thin films of *p*-CuTAPP-intercalated α-ZrP·2PMA oriented perpendicular and parallel to B_0 are presented inFigure 9. The spectra are somewhat obscured by an overlapping peak centered near 2950 G. The

(20) (a) Ungashe, S. B., Ph.D. Dissertation, Princeton University, 1991. (b) Ungashe, S. B.; Groves, J. T. *Adv. Inorg. Biochem.*, in press.
(21) Ishikawa, K. *J. Am. Chem. Soc.* **1991**, *113*, 621.
(22) Monoharan, P. T.; Rogers, M. T. In *Electron Spin Resonance of Metal Complexes*; Yen, T. F., Ed.; Plenum Press: New York, 1969; p 143.
(23) (a) Palacin, S.; Ruaudel-Teixier, A.; Barraud, A. *J. Phys. Chem.* **1986**, *90*, 6237. (b) Cook, M. J.; Daniel, M. F.; Dunn, A. J.; Gold, A. A.; Thomson, A. J. *J. Chem. Soc., Chem. Commun.* **1986**, 863.
(24) (a) Hofman, U. *Angew. Chem., Int. Ed. Engl.* **1968**, *7*, 681. (b) Alberti, G.; Casciola, M.; Constantino, U. *J. Collold Interface Sci.* **1985**, *107*, 256. (c) Burwell, D. A.; Valentine, K. G.; Timmermans, J. H.; Thompson, M. E. *J. Am. Chem. Soc.* **1992**, *114*, 4144. (d) Lee, C. F.; Myers, L. K.; Valentine K. G.; Thompson, M. E. *J. Chem. Soc., Chem. Commun.* **1992**, 201.
(25) McBride, M. B.; Pinnavaia, T. J.; Mortland, M. M. *J. Phys. Chem.* **1975**, *79*, 2430.

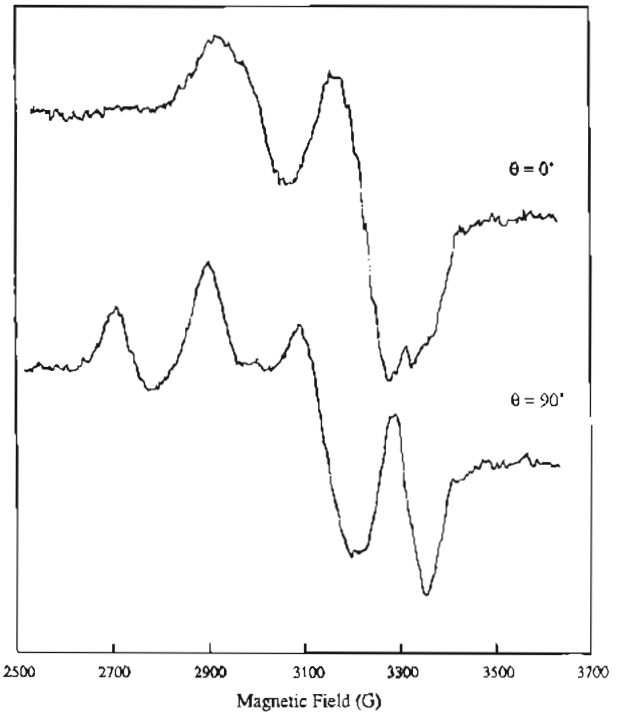

Figure 10. EPR spectra of uniaxially oriented films of $\alpha,\alpha,\alpha,\alpha$-*o*-CuTAPP-intercalated α-ZrP·2PMA oriented parallel (top) and perpendicular (bottom) to the magnetic field.

spectra are quite similar, with both parallel and perpendicular components of the Cu(II) signal being evident at the two orientations. The lack of orientational dependence of the *p*-CuTAPP intercalate is consistent with a porphyrin orientation tilted nearly 45° relative to the host layers. Together, the EPR data and 17-Å interlayer spacing of *p*-H_2TAPP- and *p*-CuTAPP-exchanged α-ZrP·2PMA are consistent with a guest layer morphology consisting of a monomolecular porphyrin layer in which the heme planes are canted nearly 45° relative to the host sheets, as depicted in Figure 5a.

By contrast, ordered EPR spectra of the *o*-$\alpha,\alpha,\alpha,\alpha$-CuTAPP intercalate, depicted in Figure 10, display a very strong orientation dependence. With the thin films oriented perpendicular to B_0 (θ = 90°), the $g_\parallel$ signal clearly dominated the EPR spectrum ($g_\parallel$ = 2.219, A = 147 G), with a characteristic four-peak pattern arising from coupling to the nuclear spin of Cu ($I_N = {}^3/_2$). A small $g_\perp$ component was also present, as evidenced by the dip in the baseline near 3200 G. Conversely, with the host layers oriented parallel to B_0 (θ = 0°), mainly $g_\perp$ was observed ($g_\perp$ = 2.062), with hyperfine coupling to the pyrrole nitrogens being visible. The predominance of $g_\parallel$ at θ = 90° and $g_\perp$ at θ = 0° indicates that the porphyrins were highly ordered relative to the host lamellae, with the heme macrocycles lying parallel to the ZrP sheets. The EPR data, in conjunction with the major phase of the *o*-$\alpha,\alpha,\alpha,\alpha$-$H_2$TAPP-exchanged complex of 19 Å, suggest that the $\alpha,\alpha,\alpha,\alpha$ derivatives intercalated in α-ZrP predominantly formed guest structures consisting of porphyrin bilayers in which the heme planes were oriented parallel to the ZrP sheets. The presence of perpendicular and parallel components in the EPR spectrum of the Cu(II) derivative obtained at 0 and 90° relative to B_0, however, indicates that the sample was not completely ordered, in accord with the presence of multiple phases in the XRD pattern of *o*-$\alpha,\alpha,\alpha,\alpha$-$H_2$TAPP-intercalated α-ZrP·2PMA. The strong orientation dependence of the Cu(II) EPR spectra, in conjuction with the predominant 19-Å phase of the *o*-$\alpha,\alpha,\alpha,\alpha$-$H_2$TAPP-exchanged complex, are consistent with a guest phase composed of a porphyrin bilayer in which the hemes lie parallel with the host lamellae.

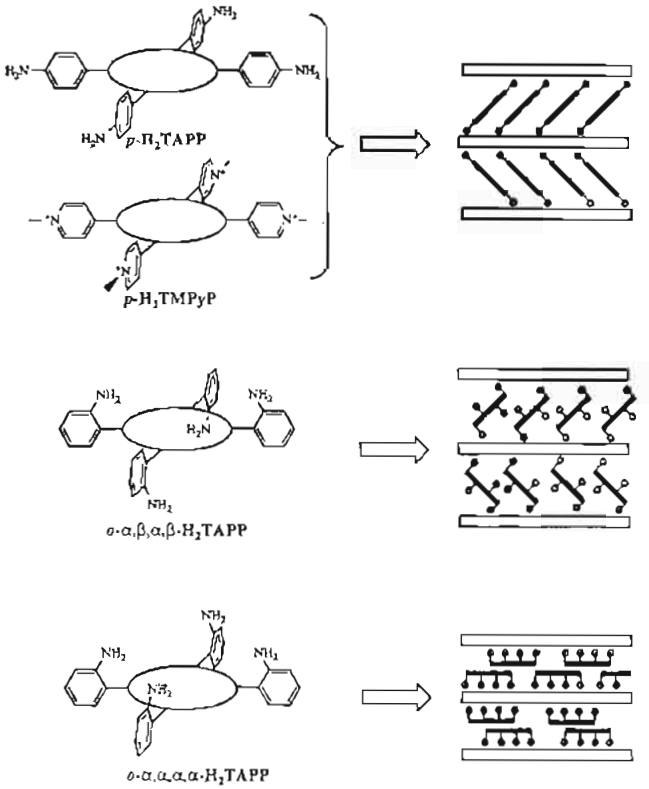

Figure 11. Proposed structures of the predominant guest phases formed upon intercalation of (a) H_2TMPyP and *p*-TAPP derivatives, (b) *o*-$\alpha,\beta,\alpha,\beta$-$H_2$TAPP, and (c) *o*-$\alpha,\alpha,\alpha,\alpha$-$H_2$TAPP

Discussion

The XRD patterns of porphyrin-exchanged α-ZrP·2PMA, in conjunction with EPR spectra of uniaxially oriented samples of Cu(II) porphyrins, indicate that the guest morphologies of amino- and pyridinium-substituted porphyrins are dictated by the location of the substituents on the *meso* aromatic rings. The interlayer spacing of 17 Å for *p*-H_2TAPP-intercalated α-ZrP·2PMA, in conjunction with the low orientational dependence of the EPR spectra of uniaxially ordered films of the *p*-CuTAPP intercalation complex, indicates that the *p*-TAPP derivatives formed guest phases consisting of a monomolecular porphyrin layer, with the heme planes tilted nearly 45° relative to the host lamellae. The similar layer spacing observed in H_2TMPyP-exchanged α-ZrP·2PMA presumably also reflects a canted monolayer guest assembly. Conversely, XRD patterns of α-ZrP·2PMA exchanged with rotational isomers of *o*-H_2TAPP revealed the formation of multiple guest structures, with the dominant phases being dependent on the identity of the atropisomer. The predominant 19-Å phase observed for *o*-$\alpha,\alpha,\alpha,\alpha$-$H_2$TAPP-intercalated ZrP·2PMA, in conjunction with the strong orientational dependence of the EPR spectra of uniaxially oriented films of the *o*-$\alpha,\alpha,\alpha,\alpha$-CuTAPP-exchanged complex, suggests that the $\alpha,\alpha,\alpha,\alpha$ derivatives predominantly formed bilayer guest structures in which the heme macrocycles were oriented parallel to the host lamellae. Conversely, the dominant 17-Å phase of the *o*-$\alpha,\beta,\alpha,\beta$-$H_2$TAPP-exchanged host implies adoption of a canted porphyrin monolayer, whereas the $\alpha,\alpha,\alpha,\beta$ isomer formed significant amounts of both tilted and planar porphyrin ensembles. The proposed structures corresponding to the dominant phases formed by the different porphyrin guests are illustrated in Figure 11.

The preferred porphyrin guest morphologies appear to be dictated by optimization of electrostatic interactions[9] and hydrogen bonding between the porphyrin amino and pyridinium substituents and the host phosphates. Considering *p*-H_2TAPP as a square with the amino groups at the vertices, the surface area is estimated to be 225 Å^2, corresponding to 56 Å^2 per amine. The

free area per phosphate OH in α-ZrP, however, is only 24 Å^2; hence, porphyrins oriented parallel to the phosphate layers are incapable of reacting with all of the hydroxyl groups on the surface of the host. In order to decrease the effective surface area per amino group, the hemes are forced to tilt relative to the host sheets, thereby presenting only the porphyrin edges to the phosphate layers. A similar canted monolayer assembly was determined for porphyrins and metalloporphyrins exchanged into clays[9,10] and was rationalized by balancing of the host charges by the guest pyridinium groups. The similar gallery heights of *p*-TAPP- and H_2TMPyP-exchanged α-ZrP·2PMA and CuTMPyP-intercalated fluorohectorite are consistent with the similar reactive site densities of the hosts. Conversely, layered hosts with low charge densities, such as montmorillonite and hectorite, can accommodate cationic porphyrins parallel to the host sheets, since the porphyrins are capable of balancing the host charges in such an orientation.[7-9] Tilting of *p*-TAPP away from being parallel to the ZrP sheets enhances the hydrogen-bonding interactions between the porphyrin amines and host phosphates. Tilting directs the amino groups toward the phosphate layers, such that all three ammonium hydrogens become available for hydrogen bonding to the phosphate lamellae. Tilted orientations have also been determined for alkylamines intercalated into α-ZrP.[14] Hydrogen bonding is not required for canting of para-substituted porphyrins in α-ZrP, however, as demonstrated by the tilted orientation adopted by H_2TMPyP.

In contrast to the case of *p*-TAPP, the amino groups of *o*-α,α,α,α-TAPP form a square above one porphyrin face, as can be seen in Figure 3. Thus, for porphyrins oriented parallel to the host lamellae, placement of the amino groups at the *ortho* phenyl positions directs them toward the phosphate sheets, favoring hydrogen-bonding interactions. Furthermore, because the amino groups of the α,α,α,α isomer reside on only one porphyrin face, assembly of a planar porphyrin bilayer could produce up to twice the number of amine–phosphate interactions per guest layer as would a planar monolayer. We surmise that the combination of the high density of amine–phosphate interactions and favorable hydrogen bonding between the guest amines and host phosphates directs the assembly of *o*-α,α,α,α-TAPP derivatives into planar porphyrin bilayers. The density of amino groups in a planar bilayer, however, is still insufficient for reaction with all of the host hydroxyls, which may account for the presence of phases at 17 and 25 Å present in the XRD pattern of the *o*-α,α,α,α-H_2-TAPP intercalation complex, which correspond to tilted heme structures.

The driving force for planar bilayer formation is not as great in the other rotational isomers: only 50% more amine–phosphate interactions are expected for a planar bilayer of α,α,α,β-*o*-TAPP compared to a planar monolayer, whereas the number of amine–phosphate interactions is expected to be the same for a planar monolayer and planar bilayer of *o*-α,β,α,β-TAPP. Hence, the amine density anticipated for a planar assembly of *o*-α,β,α,β-TAPP is only slightly greater than that for a planar monolayer of *p*-TAPP. Due to the decreasing ability of the α,α,α,β and α,β,α,β isomers to form planar structures with high amine densities, the driving force to maximize ion pairing by tilting of the porphyrins relative to the host layers increases accordingly, apparently outweighing the concomitant decrease in hydrogen bonding. This trend is illustrated by the decrease in the relative contribution of the planar porphyrin bilayer phase at 19–20 Å, from *o*-α,α,α,α-H_2TAPP to the α,α,α,β and α,β,α,β rotamers, and the concomitant increase in the 17-Å phase corresponding to a planar porphyrin monolayer. Hence, while the dominant guest phase of α,α,α,α was a planar porphyrin bilayer, *o*-α,β,α,β-H_2TAPP primarily formed a tilted monolayer guest ensemble. The orientation of some of the α,β,α,β atropisomer parallel to the phosphate sheets, despite the similar density of amine–phosphate interactions expected for analogous guest phases of isomeric *p*-TAPP, may reflect enhanced hydrogen bonding of the ortho-substituted heme in a planar orientation.

Conclusion

The specific control of porphyrin orientations is an important goal in the design of catalysts, reversible oxygen binders, and conductors. For example, cofacially arranged porphyrin dimers have been utilized for the reduction of dioxygen to water,[26] nitrogen fixation,[27] and reversible oxygen binding.[28] Cofacial and interfacial porphyrin polymers have also been synthesized as models for photoinduced charge separation.[29] The synthesis of multisite porphyrin structures, however, often proves to be challenging. We have described the preparation of spatially well-defined ensembles with controllable microenvironments by insertion of relatively simple porphyrins into ordered hosts. This approach may be useful for the development of materials custom-tailored for their specific functions.

The synthesis of porphyrin-intercalated α-ZrP by exchanging amino- and pyridinium-substituted porphyrins into the *p*-methoxyaniline-preintercalated complex α-ZrP·2PMA has been described. The compounds reported here represent the first example of the insertion of porphyrins into bulk α-ZrP. α-ZrP·2PMA is a useful starting material for the intercalation of bulky and weakly basic guests, in that it combines a large interlayer spacing with easily exchanged groups. Unlike alcohol intercalates, α-ZrP·2PMA is quite stable and can be stored as a solid under ambient conditions for long periods of time. Furthermore, the intercalation of H_2TMPyP demonstrates that the PMA derivative is also capable of participating in ion exchange reactions.

In addition, we have shown that the architecture of the porphyrin assemblies can be controlled through design of simple porphyrin guests. Monolayer and bilayer guest structures have been synthesized, with the heme guests adopting parallel or tilted orientations relative to the host layers. The morphology of the guest phases was dictated by the location of amino and pyridinium substituents residing on the *meso* aromatic groups of the hemes, with the porphyrins adopting structures which maximized host–guest electrostatic interactions and hydrogen bonding between guest amines and host phosphates. Further characterization of the *o*-TAPP intercalation complexes, as well as investigation of the reactivities of related metalloporphyrin assemblies toward oxygen binding and catalysis, is currently underway. In addition, synthesis of more stable, covalently bound porphyrin intercalated complexes is being investigated.

Experimental Section

Instruments. UV–visible spectra were recorded on a Varian-Cary 2390 or a Hewlett Packard 8452 spectrophotometer, EPR spectra on a Bruker X-band ER 200D spectrometer, and ^{1}H NMR spectra on a General Electric QE-300 spectrometer. Powder X-ray diffraction patterns were obtained on a Sintag PAD-V diffractometer using Cu *Kα* (λ = 1.5418 Å) radiation, and GC samples were assayed using a Hewlett Packard 5890 gas chromatograph.

(26) (a) Collman, J. P.; Marrocco, M.; Denisevich, P.; Koval, C.; Anson, F. C. *J. Electroanal. Chem. Interfacial Electrochem.* **1979**, *101*, 117. (b) Kim, K.; Collman, J. P.; Ibers, J. A. *J. Am. Chem. Soc.* **1988**, *110*, 4242. (c) Collman, J. P.; Hutchison, J. E.; Lopez, M. A.; Tabard, A.; Guilard, R.; Seok, W. K.; Ibers, J. A.; L'Her, M. *J. Am. Chem. Soc.* **1992**, *114*, 9869. (d) Chang, C. K.; Liu, H. Y.; Abdalmuhdi, I. *J. Am. Chem. Soc.* **1984**, *106*, 2725. (e) Ni, C.; Abdalmuhdi, I.; Chang, C. K.; Anson, F. C. *J. Phys. Chem.* **1987**, *91*, 1158.

(27) Collman, J. P.; Hutchison, J. E.; Lopez, M. A.; Guilard, R.; Reed, R. A. *J. Am. Chem. Soc.* **1991**, *113*, 2794.

(28) Guilard, R.; Lopez, M. A.; Tabard, A.; Richard, P.; Lecomte, C.; Brandes, S.; Hutchison, J. E.; Collman, J. P. *J. Am. Chem. Soc.* **1992**, *114*, 9877.

(29) (a) Schouten, P. G.; Warman, J. M.; de Haas, M. P.; Fox, M. A.; Pan, H. *Nature* **1991**, *353*, 736. (b) Wamser, C. C.; Bard, R. R.; Senthilathipan, V.; Anderson, V. C.; Yates, J. A.; Lonsdale, H. K.; Rayfield, G. W.; Friesen, D. T.; Lorenz, D. A.; Stangle, G. C.; van Eikeren, P.; Baer, D. R.; Ransdell, R. A.; Golbeck, J. H.; Babcock, W. C.; Sandberg, J. J.; Clarke, S. E. *J. Am. Chem. Soc.* **1989**, *111*, 8485.

Materials and Methods. All purchased reagents were of highest available purity and were used without further purification. All solvents were of reagent grade and were used without further purification except $CHCl_3$ and CH_2Cl_2, which were distilled from CaH_2 under argon. The tosylate and chloride salts of H_2TMPyP were purchased from Aldrich. *p*-H_2TAPP was prepared by a literature procedure which entailed synthesis of the tetrakis(*p*-nitrophenyl)porphyrin, followed by reduction to the tetraamine using anhydrous $SnCl_2$.[30] The mixed isomers of *o*-H_2TAPP were synthesized by the procedure of Collman and co-workers.[31] The $\alpha,\beta,\alpha,\beta$ and $\alpha,\alpha,\beta,\beta$ atropisomers were separated by column chromatography on silica gel, eluting with 15% EtOAc/85% $CHCl_3$. The more polar $\alpha,\alpha,\alpha,\beta$ and $\alpha,\alpha,\alpha,\alpha$ atropisomers were then eluted with 1:1 acetone/$CHCl_3$. The atropisomers were further purified by thick layer TLC on silica gel. Cu(II) porphyrins were prepared using standard procedures,[6c] although metalation of *o*-$\alpha,\alpha,\alpha,\alpha$-CuTAPP was performed at room temperature to minimize isomerization of the atropisomer.

Synthesis of α-ZrP·2PMA. α-ZrP·2PMA was prepared *via* ZrP(EtOH)$_x$ as follows. A 3.83-g sample (0.01 mol) of $Zr(O_3PO^-)_2(Na^+)_2{\cdot}3H_2O$ was suspended in 150 mL of EtOH with stirring. To this slurry was added dropwise 4.25 g of 48% HBF_4. After 24 h the solid ZrP(EtOH)$_x$ was filtered off and washed with 100 mL of EtOH; care was always taken to ensure that the solid ZrP(EtOH)$_x$ remained wet with EtOH. This ZrP(EtOH)$_x$ slurry was added to 12.3 g of *p*-anisidine dissolved in 50 mL of EtOH, and stirred for 4 weeks. The solid intercalation product was filtered off and washed with EtOH/acetone until the washings were clear. The light pink product was dried in the air. The first five 001 reflections of the final product were visible in the powder X-ray diffraction pattern, consistent with an interlayer separation of 21.7Å.

Thermogravimetric analysis of α-ZrP·2PMA in air showed a 28% weight loss between 160 and 320 °C. Further weight loss of the remaining guest along with loss of water from the condensation of the phosphate groups to form ZrP_2O_7 occurred in two stages: 320-575 °C (15%) and 575-900 °C (slow; 8%). The total observed weight loss is 51%; the expected weight loss for α-ZrP·2PMA is (49.8%).

Reactions of α-ZrP·2PMA with Porphyrins. Typical intercalation reactions involved addition of α-ZrP·2PMA (100 mg) to a solution of 50 mg of porphyrin dissolved in 20 mL of the appropriate solvent and stirring the suspension at room temperature. Intercalations of *p*-H_2TAPP and the chloride and tosylate salts of H_2TMPyP were performed in EtOH, while the *o*-H_2TAPP atropisomers and Cu porphyrins were reacted in acetone. Reaction times varied from 2 to 14 days for *p*-TAPP exchange reactions and 2 to 3 days for *o*-TAPP reactions. The porphyrin-intercalated solids were then filtered off, washed (typically with the solvent used for the reaction), and dried in air. Reactions monitored by UV and GC entailed introduction of α-ZrP·2PMA (50 mg) to a solution of 10–20 μmol of porphyrin dissolved in 25 mL of the appropriate solvent. Samples to be analyzed by UV spectroscopy were prepared by diluting a 20-μL aliquot of the reaction solution to 2 mL with the solvent of reaction. The amount of PMA released upon porphyrin intercalation was determined by GC analysis of the reaction solvent after filtration of the host solid using a SPB-20 capillary column. The column temperature was held at 50 °C for 1 min and ramped to 190 °C at a rate of 10 °C/min. The retention time of PMA was 21.6 min. PMA concentrations were determined by comparison to those of standards ranging from 0.5 to 8 mM.

EPR Spectra of Uniaxially Ordered Samples. Uniaxially oriented thin films of *p*-CuTAPP- and $\alpha,\alpha,\alpha,\alpha$-*o*-CuTAPP-intercalated α-ZrP·2PMA were prepared by casting a slurry of the appropriate porphyrin-intercalated solid in MeOH onto 3 × 12 mm glass cover slips and drying in air to form thin films. Eight slips, thus prepared, were stacked and placed into a quartz NMR tube (i.d. = 4.5 mm). EPR spectra of the uniaxially ordered samples were recorded with the film surfaces held at 0 and 90° relative to the external magnetic field. EPR spectra were recorded at 140 K using the following parameters: microwave power = 14.2 mW; microwave frequency = 9.37 GHz; modulation frequency = 100 kHz; modulation amplitude = 5 G; time constant = 82 ms; sweep time = 168 s; receiver gain = 5×10^4. The spectra were averaged over two runs.

Acknowledgment. Support of this research by the National Science Foundation (Grants CHE-8706310 and DMR-9113002) is gratefully acknowledged.

(30) Bettelheim, A.; White, B. A.; Raybuck, S. A.; Murray, R. W. *Inorg. Chem.* **1987**, *26*, 1009.
(31) Collman, J. P.; Gagne, R. R.; Reed, C. A.; Halbert, T. R.; Lang, G.; Robinson, W. J. *J. Am. Chem. Soc.* **1975**, *97*, 1427.